Acta metall. Vol. 36, No. 6, pp. 1573–1583, 1988
Printed in Great Britain.

0001-6160/88 $3.00 + 0.00

TRANSFORMATION OF Σ17 SPECIAL TILT BOUNDARIES TO GENERAL BOUNDARIES IN TIN

E. L. MAKSIMOVA, L. S. SHVINDLERMAN and B. B. STRAUMAL
Group of the Interfaces in Metals, Institute of Solid State Physics, Academy of Sciences of the U.S.S.R., Chernogolovka, Moscow District 142432, U.S.S.R.

(*Received* 4 *February* 1987; *in revised form* 1 *June* 1987)

Abstract—The form of triple junctions "special grain boundary-general grain boundary" has been employed to investigate the temperature dependence of the ratio of the surface tensions σ_{sp}/σ_g for [001] tilt boundaries in tin in the range of misorientation angles $\varphi = 25.5$–30° at temperatures $0.85\,T_m$ to T_m. The dependence of the mobility of the boundaries on the misorientation angle ($\varphi = 26$–29.5°) has been measured at six temperatures within the 0.94–$0.98\,T_m$ interval. The temperature dependence of the mobility of tilt boundaries has been studied within $\varphi = 26$–29.5°. In the given range of angles all the dependence studies demonstrate specific features at certain temperature T_c. This temperature is constant for the particular boundary and independent of the measurement technique. The data obtained suggest the conclusion that at T_c the "Σ17 special grain boundary-general boundary" phase transition occurs. The phase equilibrium line constructed from the T_c temperatures, is described well on the basis of ideas on the dislocation structure of special grain boundaries.

Résumé—On a etudié les dépendences de température du rapport de tension de la surface σ_{sp}/σ_g aux joints des grains de flexion pour l'étain. On a mesuré la valeur σ_{sp}/σ_g à la forme des joints triples "le joint des grains spécial–le joint non spécial". On a réalisé les mesures au intervalle des angles de desorientation des joints φ de 25,5 à 30° aux températures de $0{,}85\,T_m$ à T_m. On a mesuré des dependences d'orientation de mobilité des joints des grains $\varphi = 26$–$29{,}5^\circ$ aux six températures de 0,94 à $0{,}98\,T_m$. On a etudié aussi les dependences de la température de mobilité des joints des grains de flexion dans l'intervalle des angles de desorientation φ de 26 à 29,5°. On a observé des particularités sur toutes les dependences dans un certain intervalle à la température T_c. La température T_c ne dépend que l'angle de desorientation de joint des grains et ne dépend pas de la méthode de la mesure. Les données obtenues permettent de conclure que à T_c la transmission de phase "le joint des grains spécial–le joint non spécial" se passe. Une linge de l'equilibre des phases passée à travers les températures T_c a decrite bien par le modèle de structure dislocationelle des joints des grains.

Zusammenfassung—Es wurden auf den Kippkorngrenzen in Zinn Temperaturanhängigkeiten des Verhältnises von Oberflächenspannungen σ_{sp}/σ_g untersucht. Die Grösse σ_{sp}/σ_g wurde in der Form der dreifachen Stösse "spezielle Korngrenze-nichtspezielle Korngrenzen" gemessen. Die Messungen σ_{sp}/σ_g wurden im Intervall der Missorientierungswinkel der Grenzen φ von 25,5 bis 30° bei Temperaturen von $0{,}85\,T_m$ bis T_m durchgeführt. Es wurden die Orientationabhängigkeiten der Grenzenbeweglichkeit $\varphi = 26$–$29{,}5^\circ$ bei sechs Temperaturen von 0,94 bis $0{,}98\,T_m$ gemessen. Es wurden auch die Temperaturabhängigkeiten der Beweglichkeit der Kippkorngrenzen im Intervall der Missorientierungswinkel φ von 26 bis 29,5° untersucht. An allen untersuchten Abhängigkeiten im bestimmten Intervall der Winkel wurden einige Besonderheiten bei der Temperatur T_c beobachtet. Die Temperatur T_c hängt nur vom Misorientierungswinkel der Grenze ab und nicht vom Messverfahren. Die Gesamtheit der Ergebnisse erlaubt zu schliessen, dass bei T_c ein Phasenübergang geschieht: "spezielle Korngrenze-nichtspezielle Korngrenze". Die Phasengleichgewichtslinie die Temperaturen T_c geführt wurde, wird gut vom einem Model beschrieben, in dem die Versetzungsstruktur der Korngrenzen betrachtet wird.

1. INTRODUCTION

Based on the available experimental data on the structure and properties of grain boundaries it was shown [1] that special grain boundaries exist in a limited interval of temperatures and misorientation angles. The width of the misorientation-angle interval within which the boundaries possess a special structure and properties decreases exponentially with growing Σ (Σ is the reciprocal density of coincident sites). A maximal temperature of existence of special boundaries also decreases with growing Σ. Therefore at a particular temperature only the boundaries with Σ smaller than some Σ_{max} exhibit special structure and properties.

In [1] it was supposed that under the particular values of misorientation angles and temperatures one can observe the "special boundary"–"general boundary" phase transition.

The aim of this work was to investigate in detail the thermodynamical and kinetic properties of a special boundary (Σ17 in tin) for the misorientation angles and temperatures at which said phase transition could be expected.

2. EXPERIMENTAL

2.1. The surface tension of the boundaries

The phase transition on the grain boundaries must be manifested in characteristic changes of thermodynamical and kinetic properties [2]. The main thermodynamical characteristic of grain boundaries is their surface tension.

Figure 1 shows schematically the temperature dependence of the surface tension of special boundaries σ_{sp} and general boundaries σ_g. In this case $(\partial\sigma/\partial T)_g > (\partial\sigma/\partial T)_{sp}$ because general grain boundaries are less ordered and their entropy is higher:

$$(d\sigma/dT)_g \approx -S.$$

Thus boundaries with φ close to special ones may, in principle, exist in different structural modifications (see Section 4 of this paper).

Note that for one-component systems a maximal number of coexisting phases in a grain boundary equals 3 [3]. If these temperature dependences of the surface tension σ (T) for these modifications intersect below the melting temperature, a special boundary transforms to a general one. At the kind phase transition the dependences σ (T) must exhibit a bending (Fig. 1). Normally, it is not surface tension of grain boundaries $\sigma_{g.b.}$ that is measured but, rather, the ratio of $\sigma_{g.b.}$ to the crystal free surface tension (by means of thermal etching grooves [4]) or to the surface tension of other grain boundaries (from the shape of triple junctions [5]). The second method is much more accurate. Indeed the surface tension of the boundaries are close to each other, and at a small change of σ of one of the boundaries the angles at the junction vertex are drastically changed. The surface tension of the crystal surface is greater almost by a factor of 2 than $\sigma_{g.b.}$, therefore a small change of σ_s does not practically affect the value of the large angle at the vertex of the thermal etching groove.

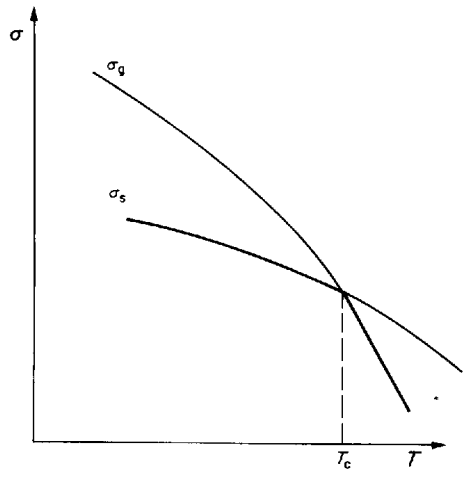

Fig. 1. Schematic presentation of the temperature dependences of the surface tension of special grain boundaries σ_{sp} and general boundaries σ_g. The first kind phase transition occurs at T_c. Above T_c the structure of general boundaries is realized, below T_c—the special boundary structure.

We have studied the ratio of the surface tension σ_{sp} of tilt boundaries with misorientation angles 25.5–30° near the special angle 28.07° (Σ17) to the surface tension σ_g, of general boundaries with misorientation angles 30–32°, lying beyond the region of the existence of Σ17 special boundaries [1]. This ratio was determined from the shape of the triple junction consisting of one special boundary and two identical general boundaries (Fig. 2). The misorientation angle $\varphi_2 = \varphi_3$ of the general boundaries was determined for the [001] boundaries from the condition $\varphi_2 = \varphi_3 = (90° - \varphi_1)/2$. The grain boundaries near coincidence misorientation Σ17 contain secondary grain boundary dislocations when $26.5° < \varphi_1 < 29.5°$ [7, 8]. So if $\varphi_2 = \varphi_3$ then angles φ_2 and φ_3 lie out of interval 26.5–29.5° when $\varphi_1 \leqslant 32°$ (see Fig. 2).

The samples with triple junctions were grown by a directed crystallization technique in high-purity argon in a high-purity graphite boat from tin with a nominal purity 99.9999 at.%. A tricrystal with a triple junction is shown schematically in Fig. 3(a). The sample with a triple junction was cut from the grown tricrystal [Fig. 3(b)]. It was chemically polished in a HNO_3–40% HF solution and placed into a high-temperature attachment to an optical microscope.

The samples were annealed in the high-purity argon, the temperature was maintained with an accuracy of ±0.3°. With successive annealing the triple junction displaced, as shown in Fig. 3. Inasmuch as $\sigma_2 = \sigma_3 = \sigma_g$, the special boundary with $\sigma_1 = \sigma_{sp}$ remained flat. The angle at the triple junction vertex was measured by means of an occularmicrometer. The values of h and l were determined [Fig. 3(b)]. In this case

$$\sigma_{sp}/\sigma_g = \sigma_1/\sigma_2 = \sigma_1/\sigma_3 = 2\cos[\text{arct}\, g(l/2h)].$$

The magnification was selected such that the measurements of h and l were conducted near the junction where the boundaries with σ_2 and σ_3 were already linear, the l/a ratio did not exceed 0.1. As shown in the work [6] the shape of the moving triple junction remains equilibrium, i.e. it is determined by the values

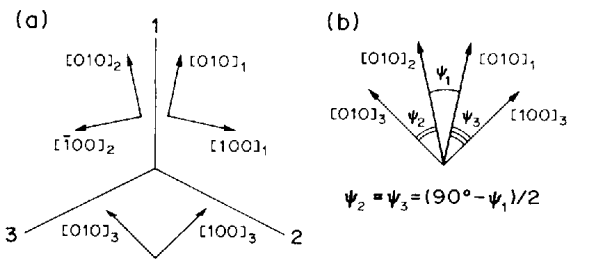

Fig. 2. Crystallography of triple junctions formed by tilt boundaries [001] which were employed to study the temperature dependences of a relative surface tension σ_1/σ_g. The junctions comprise one special boundary 1, with misorientation angle φ_1 and two identical general boundaries (2 and 3, $\varphi_2 = \varphi_3 = (90° - \varphi_1)/2$). The special boundary is shown to be lying in a (100) plane of the CSL.

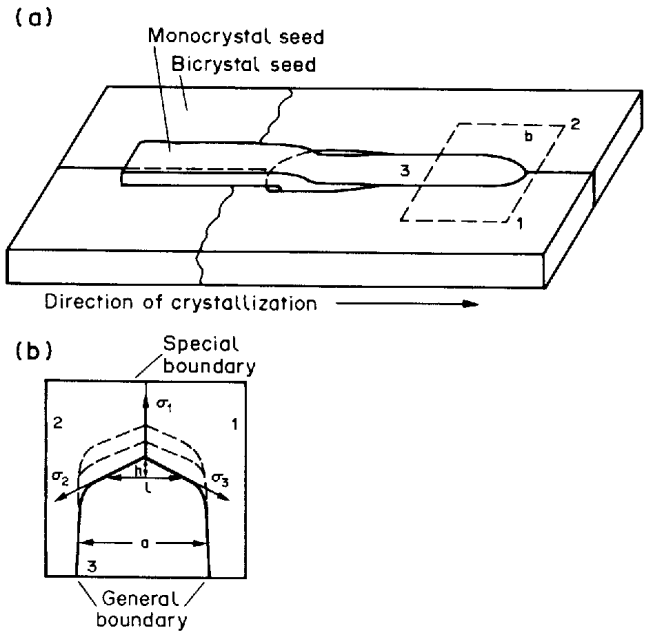

Fig. 3. The sample with triple joints. (a) The tricrystal growth scheme. (b) The sequential joints positions during measurement of temperature dependence of σ_1/σ_g. Values h and l are measured. a = const.

of σ_1, σ_2 and σ_3 if the velocity of the triple junction is limited by the grain boundary mobility rather than by the junction mobility. Figure 4 shows that the velocity of general boundaries in the junction is determined by a decrease of the driving force, acting on these boundaries, from $2\sigma_g/2q$ to $(2\sigma_g - \sigma_1)/2q$. So we measure the equilibrium value of the angle at the triple junction vertex.

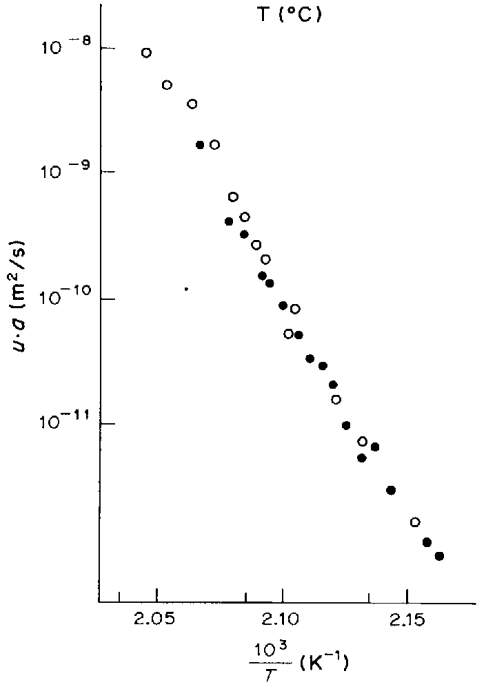

Fig. 4. Temperature dependencies of the migration rate of general boundaries (○) (boundaries 2 or 3 in Fig. 2) and of the triple junction (●). The rates are reduced to identical driving force. The rate of the triple junction is determined by the mobility of general grain boundaries and is not limited by the inherent mobility of the junction.

The geometry of the triple junctions studied was such that a change of the misorientation angle of a special boundary φ_1 the misorientation angles of general boundaries $\varphi_2 = \varphi_3$ change too. We therefore cannot plot the orientation dependence $\sigma_{sp}(\varphi)$ as we do not know how the σ_g value changes. Therefore the orientation dependence of the surface tension of tilt boundaries with $\varphi = 26.5$–$29.5°$ (at a temperature $\sim 0.97\, T_{melt}$) was determined by means of thermal etching grooves. The annealing for the groove formation was performed in a vacuum of $\sim 10^{-3}$ torr for 770 h. The profile of the thermal etching grooves was determined in 200–300 points in each sample using a microinterferometer with a laser light source, which enabled us to increase the accuracy of the measurements of σ_{sp}/σ_g.

2.2. *Boundary migration*

It was shown in the work [2–6] that the parameters of the grain boundary migration depend non-monotonically on the boundary misorientation angle. In pure metals with the impurity content from 10^{-1} to 10^{-4} at.% maxima of the boundary mobility and minima of the activation parameters of the boundary migration (activation energy, preexponential and the activation volume) are observed near special misorientation angles. These extremes were observed only on $\Sigma \leqslant \Sigma 19$ special boundaries. This is attributed to the fact [1] that the mobility measurements were conducted at rather high temperatures T/T_m, when the $\Sigma > \Sigma 19$ boundaries do not exhibit special properties.

Bicrystals for the migration parameters measurements were grown by a directed crystallization in high-purity argon in special-purity graphite boats from tin of nominal purity 99.9999 at%. Figure 5 presents schematically cutting the bicrystal for the preparation of the sample to measure the boundary mobility at a constant driving force of migration. The samples were cut in an electric-spark machine and chemically polished in a HNO_3–40% HF solution. The anneals for the mobility determination were conducted in a high-temperature attachment to an optical microscope in high-purity argon. The boundary position before and after annealing was determined by the thermal etching groove. The temperature was maintained with an accuracy of ± 0.3°C during the anneal.

3. RESULTS

3.1. The surface tension of the boundaries

We have investigated the temperature dependence of σ_1/σ_g for 10 tilt boundaries [001] in tin with misorientation angles from 25.5° to 30° at temperatures from 0.85 T_{melt} to T_{melt}. Fig. 6 demonstrates the obtained temperature dependence of σ_1/σ_g. In the figure this dependence is arranged as the misorientation angle is increased. The first two temperature dependences have the form of nearly ideal straight lines, the σ_1/σ_g ratio being close to unity. This implies that in the given temperature interval the boundaries with the misorientation angles 25.5° and 26° are general boundaries. The subsequent seven curves exhibit specific features: starting from a particular temperature the σ_1/σ_g ratio grows, reaches maximum at T_c and then decreases. These σ_1/σ_g temperature dependences exhibit the bendings. The temperature T_c increases with growing φ, reaches a maximum with $\varphi = 28.3$, close to $\varphi = 28.07°$ for $\Sigma 17$, then it decreases again. The last temperature dependence of $\sigma_1\sigma_g$ with $\varphi = 30°$ exhibits no peculiarities. The position of the bendings on the temperature dependence of σ_1/σ_g is independent of:

—the driving force of the junction motion [Fig. 7(a)]

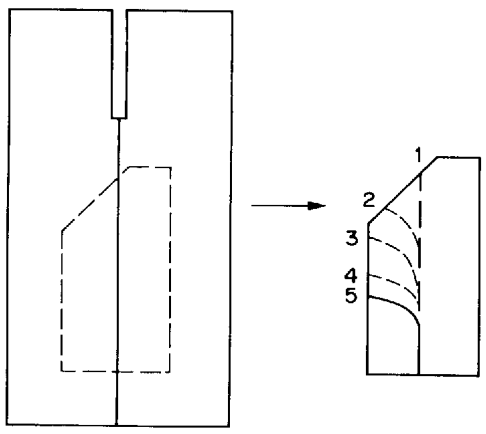

Fig. 5. Schematic presentation of a bicrystal sample for the determination of the grain boundary mobility at a constant driving force. Successive positions of the grain boundary at its migration are shown.

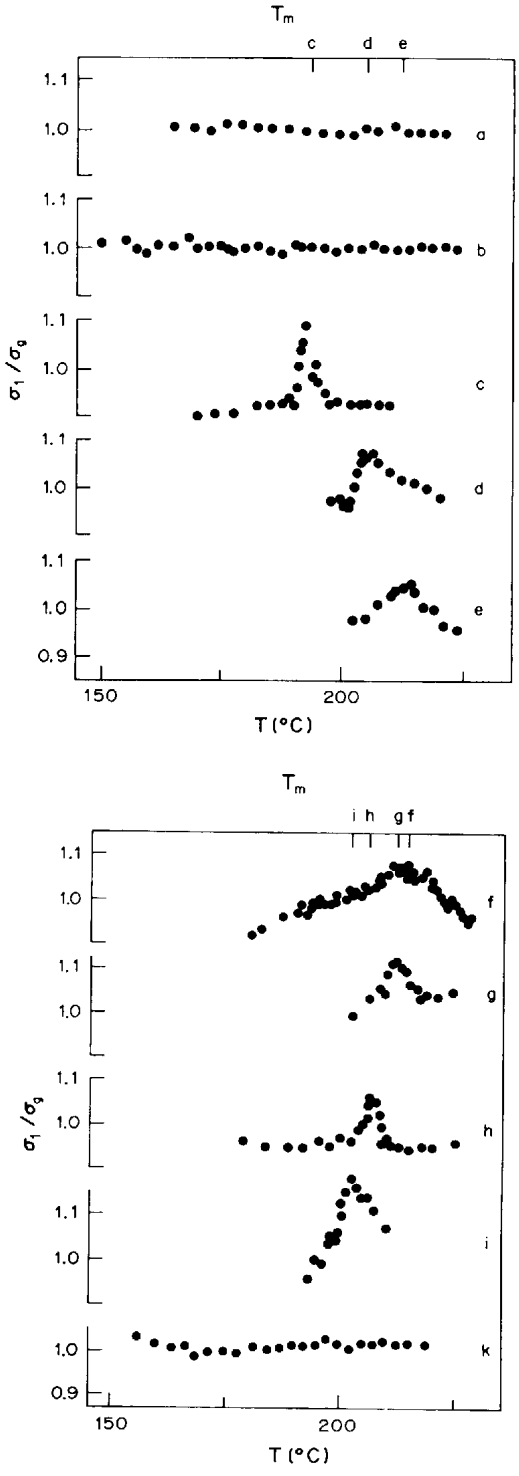

Fig. 6. Temperature dependences of the relationship between the surface tension σ_1 of special boundaries and that of general boundaries $\sigma_2 = \sigma_3 = \sigma_g$. Misorientation angles: (a) 25.5°, (b) 26.0°, (c) 26.5°, (d) 27.0°, (e) 27.7°, (f) 28.2°, (g) 28.5°, (h) 29.0°, (i) 29.5°, (k) 30.0°.

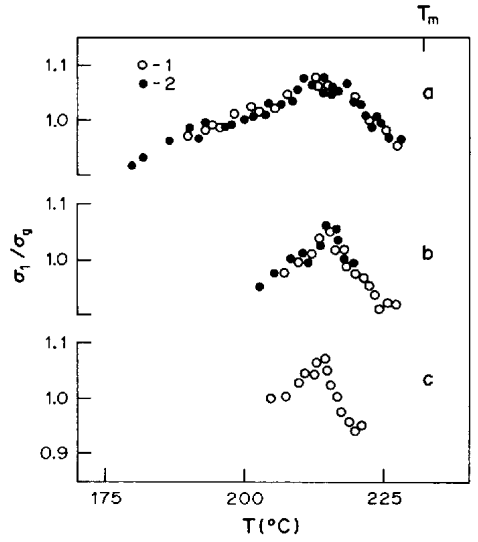

Fig. 7. (a) Temperature dependence of σ_1/σ_g (see Fig. 6) for $\varphi = 28.2°$ at different driving force: $a_1/a_2 = 2.2$. (b) Temperature dependence of σ_1/σ_g, measured at a successive increase (○) and a successive decrease (●) of the temperature for $\varphi = 28.2°$ [plane (120) CSL]. (c) The same as in (b) for $\varphi_2 \neq \varphi_3$, $\varphi_2 = 23°$, $\varphi_3 = 39°$.

—the sequence at which the temperature dependences are taken (with increase or decrease of the temperature) [Fig. 7(b)]

—misorientation angles of the general boundaries in the junction [Fig. 7 (b and c)]. So, the position of the T_c bendings on the temperature dependence of σ_1/σ_g is determined only by the misorientation angle of special boundaries with σ_1 and is independent (within the accuracy of the experiment and in the investigated interval of the parameters) of the other thermodynamical, geometrical and kinetic factors. The presence of the bendings on the temperature dependence of σ_1/σ_g implies, to our opinion, that at temperatures T_c there occurs the phase transition, that is, a Σ17 special boundary transforms to a general one. The shape of the curves in Fig. 6 fairly agrees with the schematic presentation of Fig. 1(a) for the first kind phase transition. Figure 8 presents the temperature of the T_c bending as a function of the grain boundary misorientation angle. Semicircles mark the temperature interval in which a particular boundary "behaves" as a general boundary. So, we have plotted the line separating the region of existence of Σ17 special boundaries from general boundaries. This line has the shape of a symmetric bell with the top lying at $\varphi = 28.3°$ and at a temperature of $215 \pm 2°C$ ($0.97\ T_{melt}$).

We have also studied the orientation dependence of the surface tension of the boundaries σ_1 at a temperature $T_1 = 213 \pm 2°C$, lying a little below the top of the "bell" (Fig. 8), from the shape of thermal etching grooves. This dependence is shown in Fig. 9. It has the shape of a nearly horizontal straight line with two "falling down" points. It is seen from the phase diagram on Fig. 8 that these two points exactly

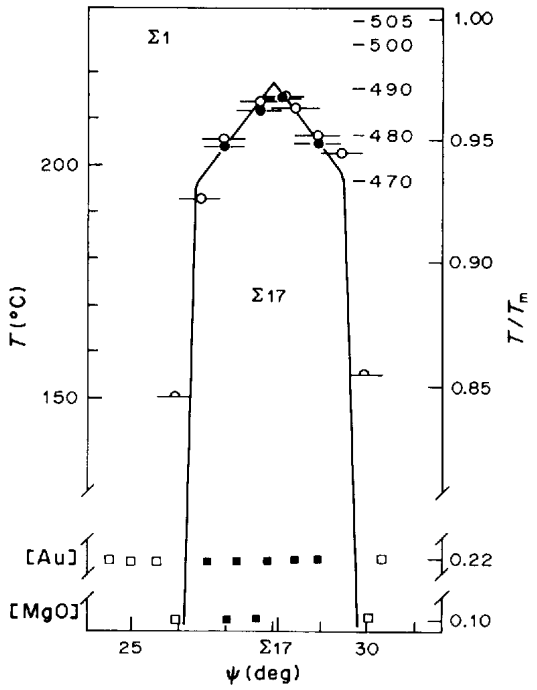

Fig. 8. Phase equilibrium like of Σ17 special boundaries and Σ1 general boundaries in tin constructed with respect to T_c. Open circles stand for the T_c values obtained by as from the temperature dependences of the surface tension [2], solid circles—from the temperature dependences of the boundary migration rate. The lower part of the figure presents the published data on the investigation of the structures of the special Σ17 twist boundaries in gold at $T/T_m = 0.2$ [12] and in magnesium oxide at $T/T_m = 0.1$ [13]. Solid squares correspond to the boundaries which exhibited secondary GBD's, open squares—to the boundaries formed by primary GBD's alone (from the diffraction data).

get to the region of existence of a Σ17 special boundary. So, the surface tension σ_{sp} of Σ17 special boundaries is below the surface tension of general boundaries σ_g at the given temperature. The value of is almost independent of the misorientation angle within the error of the measurements.

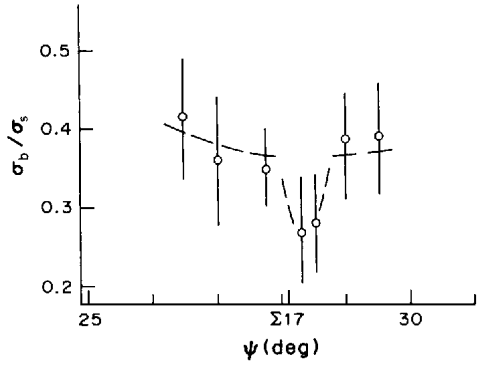

Fig. 9. Orientation dependence of the surface tension of [001] tilt boundaries in tin $\sigma_{g.b.}$ obtained by measuring the angle at the vertex of the thermal etch groove in place of the boundary occurrence on the surface. σ_{surf}—the surface tension of the (001) free surface. $T = 0.97\ T_m$.

3.2. The boundary migration

If the bendings on the temperature dependence of the surface tension σ_l/σ_g are really associated with the transformation of Σ17 special boundaries to general boundaries, then special properties of the boundaries must disappear during this event. For example, a marked difference between the mobilities of special boundaries and general boundaries must disappear.

We have studied the migration of seven [001] tilt boundaries in tin with misorientation angles from 26 to 29.5° in the temperature interval from 0.93 to 0.99 T_m. Figure 10 presents the obtained temperature dependence of the boundary mobility. The first two dependences [Fig 10(a) and (b)] have the shape of straight lines in the Arrhenius coordinates throughout the temperature interval studied. The next four temperature dependences (Fig 10(c)–(f)] exhibit a jumpwise decrease of the mobility with increasing temperature in the points T_c. Below and above T_c the mobility changes to the Arrhenius law. In the T_c point the mobility decreases with increasing temperature too by, approximately, one order. The T_c increases initially with an increase of the boundary misorientation angle [Fig. 10(c)–(d)] then, having reached the maximum [Fig. 10(e)] it drops again [Fig. 10(f)]. The last temperature dependence [Fig. 10(g)] exhibits no peculiarities.

Figure 8 presents the Σ17 and Σ1 equilibrium line obtained from bendings on the temperature de-

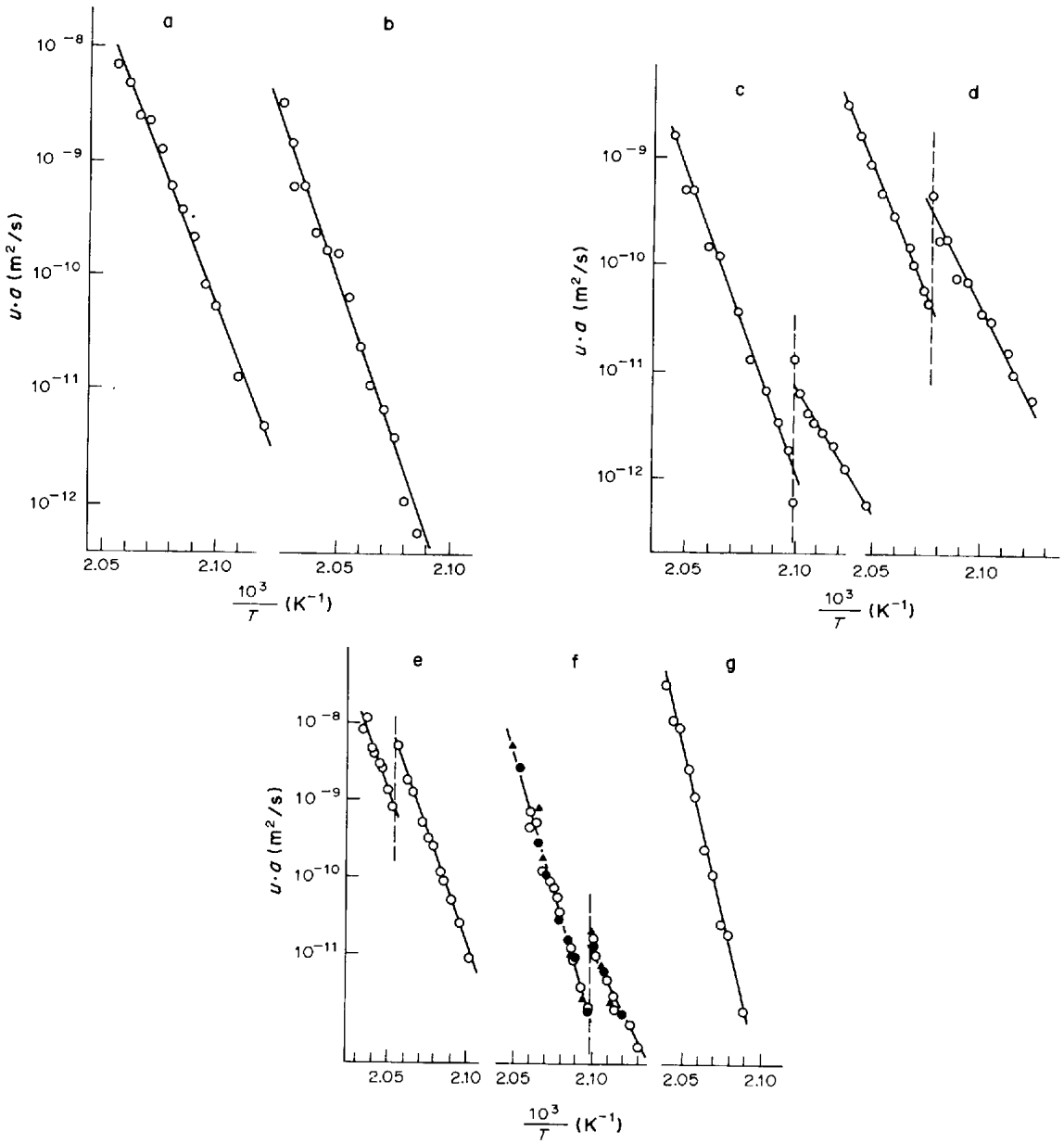

Fig. 10. Temperature dependences of the [001] tilt boundary migration rate in tin, reduced to identical driving force. Misorientation angles: (a) 26.0°, (b) 26.5°, (c) 27.0°, (d) 27.7°, (e) 28.2°, (f) 29.0°, (g) 29.5°. Fig. 2(f) presents the data for the samples with different driving force: a_1 (▲): a_2 (●): a_3 (○) = 2.9:1.5:1. T_c is seen to be independent of the migration driving force.

pendences of the surface tension. T_c temperatures at which a jumpwise change of the boundary mobility is observed are also shown in this figure. It is seen that T_c determined from the mobility jumps coincide with the $\Sigma 17$–$\Sigma 1$ transition temperatures, determined from the bendings on the temperature dependence of the surface tension. The same figure presents the published data on the investigation of the twist boundary structure in gold and magnesium oxide [7, 8]. The $\Sigma 17$–$\Sigma 1$ boundary is seen to be in the range of the angles where the images of secondary grain boundary dislocations disappear.

So the general boundaries 2 and 3 (Figs 2 and 3) in our tricrystals really are general ones. We are mentioned above (Fig. 7) that transition from $\varphi_2 = \varphi_3 = 31$ to $\varphi_2 = 23$ and $\varphi_3 = 32°$ do not shift the bending on the temperature dependence of σ_1/σ_g.

If the mobility jumps are actually associated with the equilibrium phase transition on the boundaries rather than with some kinetical processes (with the impurity effect, for example) the T_c must be independent of the driving force of the migration process. The driving force is, in dimensionality and physical sence, a pressure exerted on the boundary. In our experiments the driving force is determined by the capillary pressure of a curved grain boundary. This pressure is relatively small, namely, $\Delta F = p \approx 10^3$ Pa. It is qualitatively evident that such a small pressure cannot change appreciably the transition temperature in the condensed phase. (A quantitative estimation of T_c alteration may be performed using the Clapeyron–Klausius equation.) We shall use the characteristic values of the parameters for the phase transitions in condensed phases. The change of the phase transition temperature ΔT_c under the effect of pressure p equals $\Delta T_c \approx T_c \Delta p \, \Delta V/\lambda$. Here λ is the heat of transition, and ΔV is a change of the volume during the transition, whence $\Delta T \sim 10^{-5} K$).

The jump of the migration rate, analogous to that discussed in this work, was observed earlier on special and close to special grain boundaries in aluminium [6]. In the work [6] the jumps of the rate were attributed to the break-away of the moving boundary from the adsorbed-impurity cloud. At the break-away of the boundary from the impurity even small changes of ΔF must drastically shift the break-away temperature [9, 10]. In fact, in the simpliest version of the theory [10] the break-away occurs at an instant when the binding force of the impurity with the boundary equals the driving force of the migration.

$$\Delta F \cong \frac{2cu_0\lambda}{\lambda} \exp[u_0/kT_{Br}] \qquad (1)$$

where λ is the boundary width, c is the concentration of the impurity in the grain volume, u_0 is the binding energy of the impurity with the boundary, T_{Br} is the break-away temperature. Whence

$$\delta T_{Br} \cong -\frac{u_0}{k}\left(\ln\frac{\Delta F}{2cu_0}\right)^{-2}\frac{\delta(\Delta F)}{\Delta F}. \qquad (2)$$

From (1) and (2) we obtain

$$\frac{\delta T_{Br}}{T_{Br}} \simeq -\frac{kT_{Br}}{u_0}\frac{\delta(\Delta F)}{\Delta F}. \qquad (3)$$

For the characteristic values of the parameters ($T_{Br} \sim 10^3$ K, $u_0 \sim 50$ kJ/mol, $\delta(\Delta F)/\Delta F = 1 \div 3$) $(\delta T_{Bp}/T_{Br}) \sim 0.2$ which corresponds to the temperature shift by tens of degrees.

Figure 10(e) presents the experimental data on the T_c dependence on the driving force for the boundary with $\varphi = 29°$. In the studied range of the driving forces ($a_1 : a_2 : a_3 = 2.9 : 1.5 : 1$) the temperature of the jump is independent (within the experimental error) of the driving force. This implies that the observed jumps of the migration rate cannot be attributed to the break-away of the boundary from the impurity. Note that in the experiments dealing with the investigation of the break-away effect a change of driving force ($\Delta F \sim 10^3$ Pa) by a factor of 1.5 shifted the break-away temperature by tens of degrees [11]. Then, if the mobility jump is associated with the phase transition, its value does not have to depend on the course of intersection of the phase equilibrium line at $T = \text{const}$. or at $\varphi = \text{const}$. Figure 11 presents the orientation dependence of the mobility for four temperatures. It is seen from the figure that at the intersection of the phase equilibrium line by the trajectory $T = \text{const}$. the mobility is also change by approximately one order. This circumstance, too, confirms that we really observe the transition of one grain boundary phase to the other. Figure 12 demonstrates the superposition of the regions of $\Sigma 17$ special boundaries and general boundaries in the "reduced rate-misorientation angles" coordinates. One can

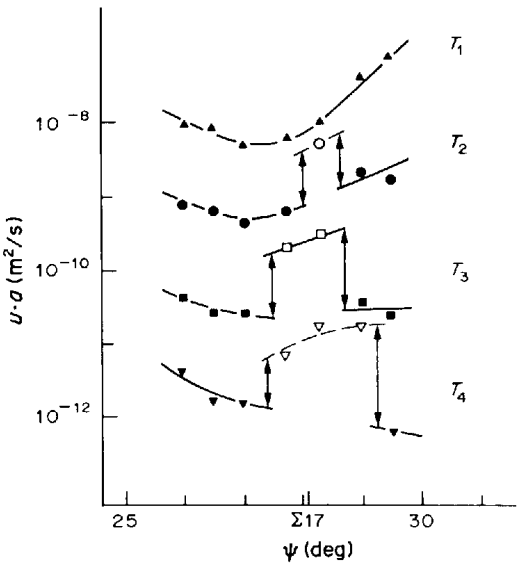

Fig. 11. Orientation dependences of the reduced migration rate for [001] tilt boundaries in tin, the misorientation angles ranging from 26 to 29.5° for different temperatures °C. (1) 218, (2) 213, (3) 208, (4) 204. The arrows show the magnitude of the reduced rate jump during the transition through the $\Sigma 17$ $\Sigma 1$ phase equilibrium line.

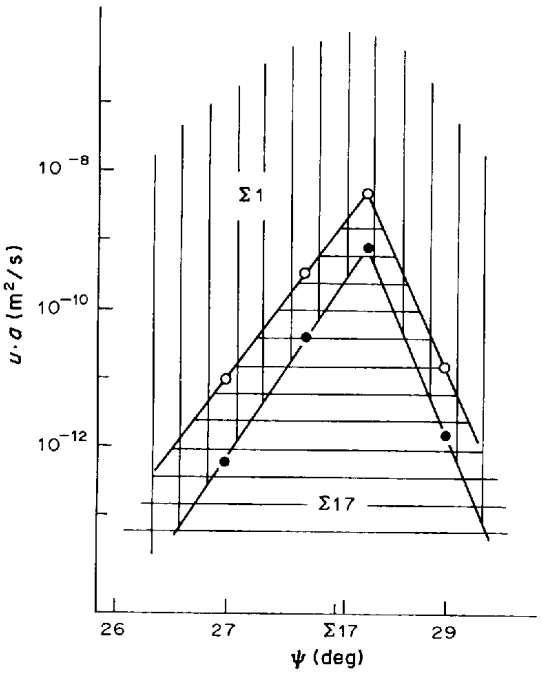

Fig. 12. Regions of reduced rates of Σ17 special boundaries and Σ1 general boundaries plotted from the data of Fig. 10. Superposition of the regions is attributed to a discontinuous decrease of the reduced rate at the transformation of Σ17 boundaries to Σ1 general boundaries.

clearly see the magnitude of the mobility jump in the place where the two regions intersect.

It is seen from Fig. 11 that at the transition of Σ17 boundaries to general boundaries the special properties of these boundaries disappear, in the region of existence of Σ17 boundaries the reduced boundary rates are higher as compared with those outside.

4. DISCUSSION

Our results on the investigation of the temperature and misorientation dependence of the surface tension and the migration rate of [001] tilt boundaries in tin near the Σ17 misorientation indicate, to our belief, the phase transformation of Σ17 special boundaries to general boundaries. The course of the temperature dependence of the surface tension σ_1 suggests that this is the first kind transition. We shall now state what boundar restructuring occur, to our mind, during this transition.

It is an experimental fact now that the grain boundary between two crystals L_1 and L_2, misoriented by an angle φ, possesses a particular ordered structure. At small misorientation angles ($\varphi \lesssim 10$–15°) the grain boundary consists of a set of lattice dislocations (networks or walls). The dislocations are separated by regions of almost ideal lattice. The spacing between the dislocations d_1, is determined by the 0-lattice period P_{01} constructed on L_1 and L_2 lattices [12]

$$C_1 = P_{01} = b_1/[2 \sin(\varphi/2)]. \quad (4)$$

Here b_1 is the length of the Burgers vector of lattice dislocations. The 0-lattice is formed by so-called equivalent sites (positions) which are not necessarily coincident with L_1 and L_2 sites. If the rotation axis is placed in any of these positions and the L_1 and L_2 lattices are rotated "back" by an angle φ, then all the L_1 and L_2 sites coincide with each other [7]. So, near the equivalent positions the L_1 and L_2 lattices are matched best, and between the equivalent positions worst. If a grain boundary is constructed between the L_1 and L_2 lattices, then as a result of the atomic relaxation grain boundary dislocations (GBDs) whose lines pass between 0-lattice points, will arise on the boundary. These dislocations are seen on electron microscopic photographs. At electron [7, 8, 14] or X-ray [15] diffraction the bicrystal, containing a grain boundary, exhibits, together with the L_1 and L_2 lattice reflections, the reflections from the grain boundary dislocation wall or network diffraction. At an increase of the grain boundary dislocation images on the electron microscopic photographs merge (with $\varphi > 15$–20° [7]). The diffraction pattern is, however, qualitatively unchanged, and the diffraction on the boundary periodic structure leads, as before, to the appearance of characteristic reflections on the electron diffractions patterns and X-ray photographs. The periodicity of the boundaries is described by the same relationship [1]. Figure 13(a) presents the results of d_1, measurements from the work [7]. The d_1 values

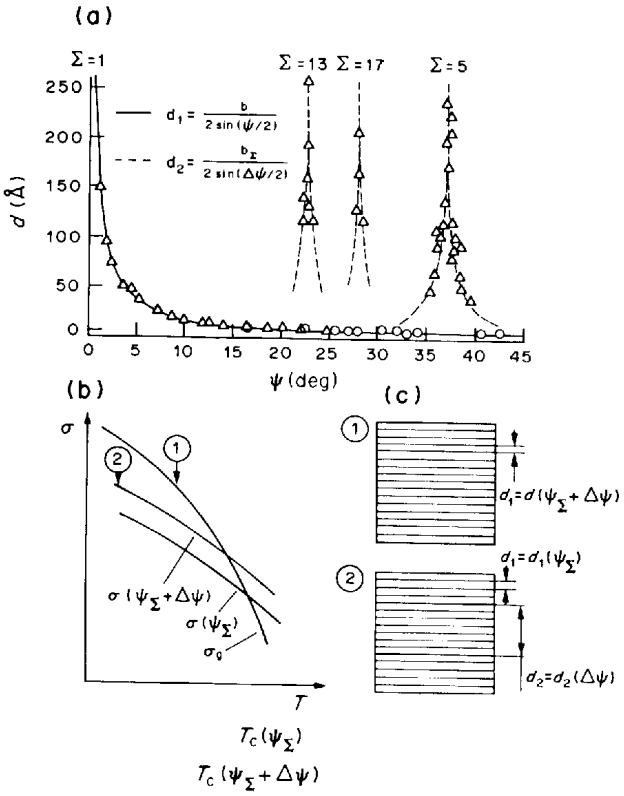

Fig. 13. (a) Spacing between primary d_1 and secondary d_2 grain boundary dislocations as a function of the misorientation angle φ, from the data of [12]. (b) Change of the surface tension.

fit well the dependence (1) (solid line). The periodic structure of grain boundaries with large misorientation angles is also observed in MgO [8]. At large misorientation angles φ the idea of individual dislocation loses its sense since at $\varphi = 15$–60° d_1 lies within 2–0.5 nm. Nevertheless the period of the network of these GBD's obeys the law (1) for all. These GBD's with the lattice Burgers vector are conventionally termed as primary grain boundary dislocations. The equilibrium boundaries, comprising only primary GBD's, will be termed as general boundaries.

So, it is an experimental fact now that at a fixed position of the grain misorientation axis and invariable position of the grain boundary with respect to the misorientation axis the structure of general boundaries is practically unvaried. The geometry of the wall or the network of the GBD, the GBD type and the Burgers vector remain constant, only the spacing between the dislocations alters. This enables us to relate such boundaries to the $\Sigma 1$ grain boundary phase (Σ is the reciprocal density of coincident sites, with $\varphi = 0$ all the L_1, and L_2 sites coincide, therefore $\Sigma = 1$).

At some values of the misorientation angle $\varphi = \varphi_{sp}$ the 0-lattice sites are coincident with the L_1 and L_2 lattice sites there form coincident site lattices with $\Sigma > 1$. In this case

$$P_{01} = \frac{m}{n} a \tag{5}$$

where a is the L_1 and L_2 lattice period. These boundaries exhibit a lower energy as compared with general boundaries [13], and their properties (mobility [3, 4], boundary diffusion parameters [2]) differ drastically from those of general boundaries. These boundaries are termed as special boundaries. Their structure is so favourable energetically that the special properties of these boundaries are preserved in the whole range of misorientation angles $2\Delta\varphi$ near a special φ_{sp}, value, though a geometrical coincidence of the L_1 and L_2 sites is disturbed at any small angular deviation from φ_{sp}. The structure of special grain boundaries is different from that of general boundaries they consist of portions of a special boundary with the structure $\varphi = \varphi_{sp}$, separated by grain boundary dislocations [see the schematic presentation of Fig. 13(b)]. The Burgers vectors of these dislocations, accommodation the φ angle deviation from the special φ_{sp}, are, however, not equal to b_1. These dislocations are termed as secondary GBD's, and their Burgers vectors are basal vectors of a so-called DSC-lattice constructed on L_1 and L_2, and misoriented by φ_{sp}. The period of the wall or the network of secondary GBD, d_2, is determined by the 0-lattice, constructed on the DSC-lattice for a particular Σ, similar to how the 0-lattice is constructed on L_1 and L_2

$$d_2 = P_{02} = b_\Sigma / [2 \sin(\Delta\varphi/2)] \tag{6}$$

The Burgers vectors b_Σ of secondary grain boundary dislocations are related to the Burgers vector of lattice dislocations by the relationship

$$b_\Sigma = b_1 / \sqrt{\Sigma}. \tag{7}$$

The secondary GBD's are seen on the electron microscopic photographs of special grain boundaries [7, 8, 14], however the electron of X-ray diffraction on the networks of these GBD's was not observed so far. For all the cases of observation of secondary GBD's, the spacing between them obeyed the relationship (3) [dashed lines in Fig. 13(c)]. Note, that the spacing between secondary GBD's, observed on special boundaries, makes up 50–250 Å, and it exceeds by 5–20 times that between primary GBD's in the regions with $\varphi = \varphi_{sp}$ and on general boundaries.

So, the structure of special grain boundaries is principally different from the general boundary structure: the portions of the boundary constructed from primary GBD's with the period $c_1 = d_1(\varphi_{sp}) = b$ alternate with secondary GBD's whose Burgers vectors are smaller than those of primary GBD's and determined by the Σ value. This difference indicates the existence for each Σ value of its own grain boundary phase, for example $\Sigma 5$, $\Sigma 13$, $\Sigma 17$ etc.

We shall explain what we mean by the grain boundary phase. At the electron or X-ray diffraction on the periodic boundary structure there arise rod-shaped reflections whose length is unambiguously related to the thickness of the disorted boundary layer. The results of the measurements [14, 15] show that the grain boundary thickness does not exceed the spacing d_1 and it is close to one or two interatomic spacings. This implies that the boundary thickness is approximately the same as the thickness of the distorted layer near the free surface of the crystal of the thickness of the adsorbed atoms monolayer on the free surface. In this sense the idea of "2D grain boundary phase" is close to "2D surface phase". An important difference consists in the fact that the 2D surface phase is "fixed" to a three-dimensional crystal from one side, whereas the two dimensional boundary phase is between three-dimensional crystals.

It follows from the above said that at a particular value of the misorientation angle φ close to special

$$\varphi = \varphi_{sp} + \Delta\varphi$$

two different boundary structures can, in principle, be realized [see Fig. 13(c)]: involving primary dislocations alone with the period d_1 [Fig. 13(c), solid line]

$$d_1 = d_1(\varphi = \varphi_{sp} + \Delta\varphi) = b_1 / [2 \sin(\varphi/2)]$$

or consisting from special-boundary portions with the periodicity

$$d_{1sp} = d_1(\varphi_{sp}) = b_1 / [2 \sin(\varphi_{sp}/2)]$$

separated by secondary grain boundary dislocations with the period

$$d_2 = d_2(\Delta\varphi) = b_\Sigma/[2\sin(\Delta\varphi/2)]$$

[Fig. 13(c), dashed line].

Of the two structure that one is realized whose free energy is lower. With an increase of $\Delta\varphi$ the energy of the secondary-dislocation wall is increased, and at a specific $\Delta\varphi$ the type of the boundary structure changes. Such a change of the structure must, to our mind, have a character of the phase transition. The "special boundary-general boundary" transition may be observed with temperature variation as well, since the free energy of less orgered general boundaries decreases with the temperature more rapidly than that of special boundaries. As it has been noted, the course of the temperature dependence of the surface tension of the grain boundaries investigated suggests that the $\Sigma17$–$\Sigma1$ transition occurs according to kind I. We shall analyze the theormodynamics of this transition and on the base of the ideas of the boundary dislocation structure we shall plot the $\Sigma17$ and $\Sigma1$ phase equilibrium line in the T-φ coordinates.

Consider the equilibrium of two grain boundary phases in a one-component system. The Gibbs equation of adsorption for the two coexisting boundary phases is

$$\begin{cases} d\sigma_1 = -S_1^S\,dT - \Gamma_1\,d\mu + \left(\dfrac{\partial\sigma}{\partial\varphi}\right)_1 d\varphi \\ d\sigma_2 = -S_2^S\,dT - \Gamma_2\,d\mu + \left(\dfrac{\partial\sigma}{\partial\varphi}\right)_2 d\varphi \end{cases}$$

Γ_1 and Γ_2—autoadsorption; S_1^S, S_2^S—the boundary entropy excess pro unit area. Both boundary phases are in equilibrium with volume phase

$$d\mu = d\mu_v = -S_v\,dT$$

μ—chemical potential; S_v—the entropy excess for one excess atom. In equilibrium $d\sigma_1 = d\sigma_2$, so

$$(S_v\Gamma_1 - S_1^S)\,dT + \left(\frac{\partial\sigma}{\partial\varphi}\right)_1 d\varphi = (S_v\Gamma_2 - S_2^S)\,dT + \left(\frac{\partial\sigma}{\partial\varphi}\right)_2 d\varphi$$

and

$$\frac{dT}{d\varphi} = \frac{(\partial\sigma/\partial\varphi)_1 - (\partial\sigma/\partial\varphi)_2}{(S_v\Gamma_2 - S_2^S) - (S_v\Gamma_1 - S_1^S)} = \frac{(\partial\sigma/\partial\varphi)_1 - (\partial\sigma/\partial\varphi)_2}{\dfrac{S_1^S - S_v}{a_1} - \dfrac{S_2^S - S_v}{a_2}}$$

where a_1, a_2—specific area, occupied in the boundary by mole of the material. The a_1 and a_2 in all boundaries are nearly equal ($a_1 \approx a_2 \approx A$). The angular dependence of σ for general boundary is very weak, so $(\partial\sigma/\partial\varphi) \approx 0$. Then

$$\frac{dT}{d\varphi} \approx \frac{A(\partial\sigma/\partial\varphi)_1}{\Delta S_1^S - \Delta S_2^S} = \frac{A}{\Delta S^S}\left(\frac{\partial\sigma}{\partial\varphi}\right)_1.$$

A change of a special boundary misorientation angle by $\Delta\varphi$ gives rise to a wall of secondary GBD's with the period on the boundary. The surface tension of tilt boundaries increases by $\Delta\sigma$ in this case

$$\Delta\sigma = \frac{Gb_\Sigma}{4\pi(1-\nu)}\cdot\sin\Delta\varphi\left(1 + \ln\frac{b_\Sigma}{2\pi r_0} - \ln\Delta\varphi\right).$$

Here r_0 is a cutting radius, and G and ν are elastic moduli. Then (for small temperature intervals ΔT)

$$\Delta T = -\frac{A}{\Delta S^S}\left[\frac{GB_\Sigma\sin\Delta\varphi}{4\pi(1-\nu)}\left(1 + \ln\frac{b_\Sigma}{2\pi r_0} - \ln\Delta\varphi\right)\right].$$

In Fig. 14 our dependence of T_c on misorientation angle φ (Fig. 3) is plotted in the coordinates $(\Delta T/\sin\Delta\varphi) - (\ln\Delta\varphi)$. One can determine the value of r_0 from the segment cut off on the abscissa axis: $r_0 = 5b_\Sigma$. So, the width of secondary grain boundary dislocation cores exceeds by several times their Burgers vector. This agrees with the ideas of a great width of grain boundary dislocation cores, suggested in [16]. The angle $\Delta\varphi^*$ at which grain boundary dislocation cores coalesce can be estimated from the condition $d_2 = 2r_0$. Then $\Delta\varphi^* \sim 6°$.

From the slope of the straight line of Fig. 14 one can estimate the value of $A/\Delta S^S$. With $G = 18$ GPa [17], $\nu = 0.330$ [17] and $b_\Sigma = a/\sqrt{17} = 7.8\cdot10^{-2}$ nm. We obtain $\Delta S^S/A = 3\cdot10^{-4}$ J/m^{2}K. The value of $\Delta S^S/A$ can also be estimated from general thermodynamical considerations $\Delta S = L/T_0$. For tin melting $L_m/T_0 = 14$ J/mol K [17] $A = V_{mol}/a = 3\cdot10^{-4}$ m^2/mol [17]. We obtain $\Delta S^S/A = 4\cdot10^{-4}$ J/m^2 K. So, the value of $\Delta S^S/A$ obtained in our experiments for the $\Sigma17 - \Sigma1$ transition agrees with the estimations for a typical bulk phase transition.

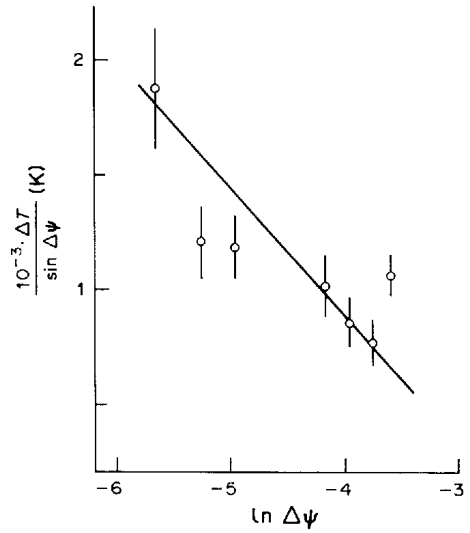

Fig. 14. Correspondence of the $\Sigma17$ $\Sigma1$ equilibrium line (dots, from the data of Fig. 10) to the dislocation model for the transition temperature T_c (solid line). φ—is the misorientation angle, $\Delta T = 220\,°C - T_c$.

We mean that transition "special grain boundary-general boundary" is not unique possible phase transition in grain boundaries. Recently it was shown that addition of second component (Au) could modify the structure of low angle boundaries in Fe [18]. This is undoubtely the compositional grain boundary phase transition. The results of computer simulation show the multiplicity of possible grain boundary structure at fixed misorientation parameters [19–21]. However unlike the many computer simulation results the grain boundary dislocation model is the most simple one which describe very well the whole array of experimental data.

5. CONCLUSIONS

1. So the temperature dependences of a relative surface tension of tilt boundaries [001] in tin with misorientation angles close to 28.07° is studied for the Σ17 coincident site lattice. It is shown that near the coincidence misorientation some of these dependences exhibit bendings whose position is determined by the boundary misorientation angle. It is concluded that these bendings are due to the phase transition Σ17 special boundary–Σ1 grain boundary.

2. The temperature dependences of the migration rate are studied for tilt boundaries with the misorientation angle close to 28.08° (Σ17 CSL). It is shown that the temperature dependences of boundary migration rate exhibit jumps of the rate at T_c near the coincidence misorientation. The temperatures T_c are coincident with temperatures of the phase transitions of Σ17 special boundaries to Σ1 general boundaries, obtained in the investigation of the temperature dependences of the surface tension of these boundaries [2].

3. The temperatures T_c and the data of the work [2] are employed to plot the phase diagram of the Σ17 boundaries existence.

4. The shape of the Σ17–Σ1 phase equilibrium line agrees with the dislocation presentations of the structure of special grain boundaries.

Acknowledgements—The authors are grateful to E. I. Rabkin and S. I. Prokof'ev for the useful discussion of the work.

REFERENCES

1. L. S. Shvindlerman and B. B. Straumal, *Acta metall.* **33,** 1735 (1985).
2. A. N. Aleshin, B. S. Bokstein, A. L. Petelin and L. S. Shvindlerman, *Metallofizika* **2,** 83 (1980).
3. E. M. Fridman, Ch. V. Kopezky and L. S. Shvindlerman, *Z. Metallk.* **60,** 533 (1975).
4. B. Yu. Aristov, Ch. V. Kopezky and L. S. Shvindlerman, in *Scientific Basic of Physical Metallurgica*, p. 84 (1981). In Russian.
5. D. M. Molodov, B. B. Straumal and L. S. Shvindlerman, *Scripta metall.* **18,** 207 (1984).
6. V. Yu. Aristov, Ch. V. Kopezky and L. S. Shvindlerman, *Scripta metall.* **11,** 109 (1977).
7. T. Y. Tan, S. L. Sass and R. W. Balluffi, *Phil. Mag.* **31,** 575 (1975).
8. C. P. Sun and R. W. Balluffi, *Phil. Mag.* **A46,** 49 (1982).
9. J. W. Cahn, *Acta metall.* **10,** 789 (1962).
10. K. Lücke and K. Detert, *Acta metall.* **5,** 628 (1957).
11. B. Yu. Aristov, Ch. V. Kopezky, D. A. Molodov and L. S. Shvindlerman, *Fizika tverdogo tela* **22,** 3247 (1980).
12. W. Bollmann, *Crystal Defects and Crystalline Interfaces*, p. 316. Springer, Berlin (1970).
13. G. Hasson, J.-Y. Boos and I. Herbeuval, *Surf. Sci.* **31,** 115 (1972).
14. V. S. Postnikov, B. M. Ievlev, K. S. Solov'ev and C. B. Kushev, *Fizika metall. metalloved.* **42,** 300 (1976).
15. P. D. Bristowe and S. L. Sass, *Acta metall.* **28,** 575 (1980).
16. H. Gleiter, *Scripta metall.* **11,** 305 (1977).
17. Properties of elements, *M. Metallurgia* (1985).
18. K. E. Sickafus and S. L. Sass, *Acta metall.* **35,** 69 (1987).
19. U. Guillopé, *J. Physique* **47,** 1347 (1986).
20. J. Hasson, Y. Oh, V. Vitek and F. W. Schapink, *Trans. Japan Inst. Metals Suppl.* **27,** 285 (1986).
21. G. J. Wang, D. Schwartz, Y. Oh and V. Vitek, *Trans. Japan Inst. Metals Suppl.* **27,** 155 (1986).